

Analyst

Accepted Manuscript



This is an *Accepted Manuscript*, which has been through the Royal Society of Chemistry peer review process and has been accepted for publication.

Accepted Manuscripts are published online shortly after acceptance, before technical editing, formatting and proof reading. Using this free service, authors can make their results available to the community, in citable form, before we publish the edited article. We will replace this *Accepted Manuscript* with the edited and formatted *Advance Article* as soon as it is available.

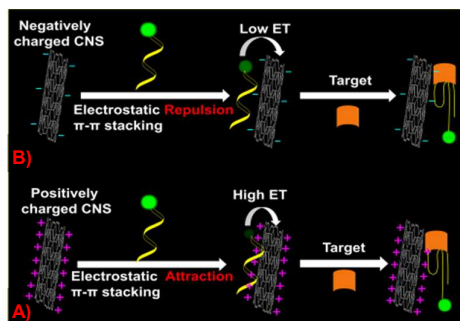
You can find more information about *Accepted Manuscripts* in the [Information for Authors](#).

Please note that technical editing may introduce minor changes to the text and/or graphics, which may alter content. The journal's standard [Terms & Conditions](#) and the [Ethical guidelines](#) still apply. In no event shall the Royal Society of Chemistry be held responsible for any errors or omissions in this *Accepted Manuscript* or any consequences arising from the use of any information it contains.

Improving Fluorescence Detection Limit with Positively Charged Carbon Nanostructure as a Low Background Signal Platform

Xiulan He, Li Zhang, Hetong Qi, Ping Yu, Junjie Fei, Lanqun Mao

Table of Content



We have demonstrated a new strategy to improve the fluorescence detection limit by enhancing the energy transfer efficiency between carbon structures and fluorescent dye using polyimidazolium-functionalized carbon nanostructures as a low background signal platform.

Cite this: DOI: 10.1039/c0xx00000x

www.rsc.org/xxxxxx

ARTICLE TYPE

Improving Fluorescence Detection Limit with Positively Charged Carbon Nanostructure as a Low Background Signal Platform

Xiulan He,^{a,b} Li Zhang,^b Hetong Qi,^b Ping Yu,^{b,*} Junjie Fei,^{a,*} Lanqun Mao^{b,*}

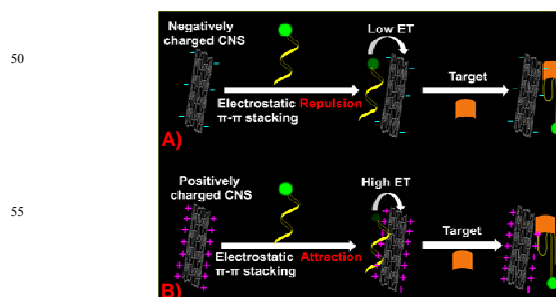
Received (in XXX, XXX) Xth XXXXXXXXXX 20XX, Accepted Xth XXXXXXXXXX 20XX

DOI: 10.1039/b000000x

We have demonstrated a new strategy to improve the fluorescence detection limit by enhancing the energy transfer efficiency between carbon structures and fluorescent dye using polyimidazolium-functionalized carbon nanostructures as a low background signal platform. Based on this, a highly sensitive method for thrombin was proposed with detection limit as low as 2.79 pM without any amplification.

The integration of the unique physiochemical property of nanostructures with bio/chem recognition unit has created new opportunities for development of sensitive and selective bioanalytical methods.¹⁻² As a one family in nanomaterials, carbon nanostructures (CNS) have attracted much attention in developing various kinds of biosensors for bioanalysis and clinical diagnosis.¹ Recently, a promising application of CNS in sensing strategy is the solution fluorescent detection due to their excellent ability in fluorescence resonance energy transfer (FRET), in which CNS could be used as good energy acceptors to quench the fluorescence of dyes.³ To this end, various kinds of CNS, including carbon nanotubes,^{4c} graphene,^{4b} graphene oxide,^{1a} carbon nanosphere^{4f} and carbon nanohorn,^{4e} have been used for developing the biosensors by integration of their fluorescence quenching property with the high selectivity of the bio/chem recognition units, e.g., peptide^{4c} and aptamers.^{4b-4d,4f} Unfortunately, all the CNS-based fluorescence biosensors reported so far have been based on the pristine CNS,⁴ in which the surface of CNS always bear negative charges (i.e., the intrinsic carboxyl groups^{4c-4e} or externally addition of negatively charged surfactant,^{4b}) to keep CNS well dispersed in aqueous solution. These negative charges weaken the interaction between dye-labeled DNA and CNS because of the electrostatic repulsion interaction, and further decrease the quenching efficiency for the dye-labeled DNA, even though the existence of π - π interaction between DNA and CNS results in the fluorescence quenching,⁵ as shown in Scheme 1A. Avoiding this electrostatic repulsion interaction would increase the quenching efficiency and thus lower the background signal, further increasing the sensitivity of the biosensors.

To accomplish this pursuit, we herein demonstrate a new strategy to improve the performance of the fluorescence biosensor by rationally introducing positive charges on the surface of the CNS. These positive charges would enhance, rather than weaken, the interaction between DNA and CNS, as shown in Scheme 1B. This enhancement, along with the π - π interaction between DNA and CNS, increases quenching efficiency of CNS towards the dye-labeled DNA, which could provide a low background signal for the biosensor and further increase the sensor sensitivity.



Scheme 1. Schematic illustration of the strategies for fluorescence aptasensors based on pristine carbon nanostructures (CNS) (A) and the Pim-functionalized CNS (B).

and CNS, as shown in Scheme 1B. This enhancement, along with the π - π interaction between DNA and CNS, increases quenching efficiency of CNS towards the dye-labeled DNA, which could provide a low background signal for the biosensor and further increase the sensor sensitivity.

To demonstrate the feasibility of this principle, carbon nanotubes (CNTs) were chosen as the model CNS and the FAM-labeled thrombin aptamer (FAM-TA) as the recognition unit. The polyimidazolium-functionalized CNTs (Pim-CNTs) were synthesized by surface-initiated atom transfer radical polymerization (Fig. S1). XPS and FTIR results suggest the successful functionalization of CNTs with Pim (Figs. S2 and S3).

To investigate the fluorescence sensor application of the prepared Pim-CNTs, we studied the change in the fluorescence intensity of FAM-TA caused by Pim-CNTs and thrombin. Fig. 1 shows the fluorescence emission spectra of 20 nM FAM-TA, which exhibits strong fluorescence emission owing to the presence of FAM (black curve). After the addition of 20 μ g/mL Pim-CNTs into the solution of FAM-TA, the fluorescence was efficiently quenched (about 96%, magenta curve). Upon its further incubation with 270 pM thrombin for 10 min, the solution exhibits significant fluorescence enhancement (dark yellow curve). Note that, both solutions of thrombin and Pim-CNTs do not emit any obvious fluorescence (green and blue curves). Thus, the increase in the intensity of the signal was due to the interaction of FAM-TA with thrombin. Moreover, the addition of thrombin into the solution of FAM-TA did not result in the change of fluorescence intensity (red curve), suggesting that the

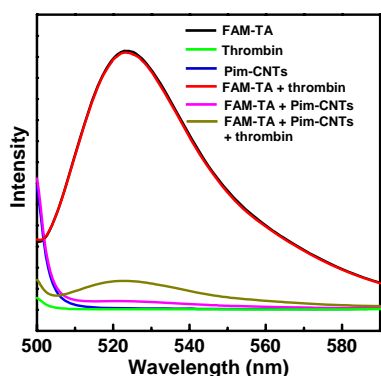


Fig. 1 Fluorescence spectra of FAM-TA (black curve), thrombin (green curve), Pim-CNTs (blue curve), FAM-TA in the presence of thrombin (red curve), FAM-TA in the presence of Pim-CNTs (magenta curve), and FAM-TA in the presence of Pim-CNTs and thrombin (dark yellow curve). FAM-TA concentration: 20 nM; Thrombin concentration: 270 pM; Pim-CNTs concentration: 20 $\mu\text{g}/\text{mL}$; λ_{ex} : 490 nm. Measurements were performed in Tris-HCl buffer (10 mM, 0.2 M NaCl, pH 7.4).

method demonstrated here was potentially useful for the quantitative determination of thrombin, as demonstrated below.

Based on the phenomena observed above, we developed a fluorescent biosensing platform for thrombin detection using the Pim-CNTs as the background signal platform. Fig. 2A shows the fluorescence intensity of the FAM-TA in the presence of 20 $\mu\text{g}/\text{mL}$ Pim-CNTs with the addition of different concentrations of thrombin. The intensity increases with increasing the concentration of thrombin and is linear with the concentration of thrombin within the concentration range of 27 - 162 pM ($F/F_0 = 0.0129C_{\text{thrombin}}(\text{pM}) + 1.073$, $R = 0.998$). In a control experiment, we did not find significant change in fluorescence intensity when thrombin was added into the pure solution of FAM-TA (i.e., without Pim-CNTs) (Fig. 2B, red circle). This control experiment again suggests that the fluorescence recovery was induced by the interaction between thrombin and FAM-TA, in which the distance between FAM and Pim-CNTs was increased and the fluorescence was recovered, as illustrated in Scheme 1B.

The limit of detection (LOD) of the aptasensor was calculated to demonstrate the advantage of the present strategy. The LOD ($S/N = 3$) was determined to be 2.79 pM, which is much lower

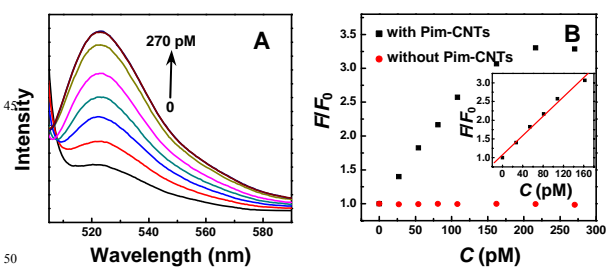


Fig. 2 (A) Fluorescence spectra of the aptasensor upon addition of different concentrations of thrombin: 0, 27, 54, 81, 108, 162, 216, 270 pM (from inner to outer). (B) Relative fluorescence changes (F/F_0) as a function of thrombin concentration for the aptasensor with (black square) and without (red circle) Pim-CNTs. Inset: calibration plot of F/F_0 versus the concentration of thrombin. F_0 and F are the fluorescence intensity for the aptasensor without and with thrombin, respectively. FAM-TA concentration: 20 nM; λ_{ex} : 490 nm; and λ_{em} : 523 nm.

Table 1. Comparison of different methods for thrombin detection.

Carbon Nanostructures	Probe	LOD	Refs.
Carbon Nanoparticles (CNPs)	TA-UCPs	0.18 nM	4a
Graphene	FAM-TA	31.3 pM	4b
SWCNTs	FAM-TA	1.8 nM	4c
Graphene Oxide	FAM-TA	2 nM	1a
Carboxylic CNPs	FAM-TA	5 nM	4d
Single Walled Carbon Nanohorn	FAM-peptide	100 pM	4e
Carbon nanosphere	FAM-TA	0.5 nM	4f
Pim-CNTs	FAM-TA	2.79 pM	This work

than those reported so far with CNS as the background signal platform, as listed in Table 1. This strategy opens a new avenue to development of highly sensitive method for thrombin determination.

To further investigate the mechanism for the low LOD of the aptasensor developed here, the quenching efficiency of the Pim-CNTs and traditional acidic-treated CNTs (at-CNTs) was compared. As shown in Fig. 3A, both kinds of CNTs could quench the fluorescence of FAM-TA. However, the Pim-CNTs show a higher quenching efficiency than the at-CNTs. For example, more than 95% of fluorescence was quenched by the addition of 16 $\mu\text{g}/\text{mL}$ Pim-CNTs into 20 nM FAM-TA solution (Fig. 3A, black square). This efficiency is almost 2-folded higher than that of at-CNTs that bears some negative charges on the surface (Fig. 3A, red circle). Since the Pim-CNTs show better solubility into the aqueous solution than the at-CNTs (Fig. 3B, vial 1 and vial 2), we thus studied the effect of such solubility difference on the quenching efficiency by using SDS-dispersed CNTs (SDS-CNTs) as a control due to its good solubility in aqueous solution (Fig. 3B, vial 3). We found that the SDS-CNTs show almost the same quenching efficiency as the at-CNTs (Fig. 3A, blue triangle), ruling out the contribution of the solubility on the high quenching efficiency observed with the Pim-CNTs. We thus considered the high quenching efficiency of the Pim-CNTs to be the consequence of noncovalent binding of FAM-TA onto the Pim-CNTs. That is, the electrostatic attraction between positively charged Pim-CNTs and negatively charged FAM-TA guarantees the close proximity of FAM with CNTs to further promote the π - π stacking interaction between FAM-TA and Pim-CNTs, leading to a high fluorescence quenching efficiency. Besides, the sole addition of Pim into the solution of

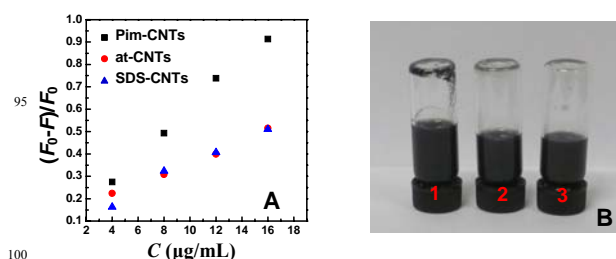


Fig. 3 (A) Fluorescence intensity versus the concentrations of Pim-CNTs (black square), at-CNTs (red circle) and SDS-CNTs (blue triangle). F_0 and F are the fluorescence intensity for the FAM-TA without and with Pim-CNTs, at-CNTs or SDS-CNTs, respectively. Measurements were performed in 0.01 M Tris-HCl buffer containing 0.2 M NaCl (pH 7.4). λ_{ex} : 490 nm. (B) Digital photographs of the at-CNTs (vial 1), Pim-CNTs (vial 2) and SDS-CNTs (vial 3) solubilized into water.

FAM-TA did not result in the decrease of fluorescence intensity (data not shown), showing that the fluorescence quenching is originated from the energy transfer between FAM and CNTs, rather than the Pim. This high energy transfer efficiency essentially leads to the low limit of detection, as listed in Table 1.

In addition to the low LOD, we found that the aptasensor was also selective, which was investigated with BSA, Cu^{2+} , Mg^{2+} , and Zn^{2+} since these species exist in blood with high concentrations. When the aptasensor was incubated for 10 min separately with 300 nM BSA, 1 μM Cu^{2+} , 1 μM Mg^{2+} , and 1 μM Zn^{2+} , we did not observe obvious change in the fluorescence intensity (data not shown), while a significant fluorescence recovery was observed with 270 pM thrombin.

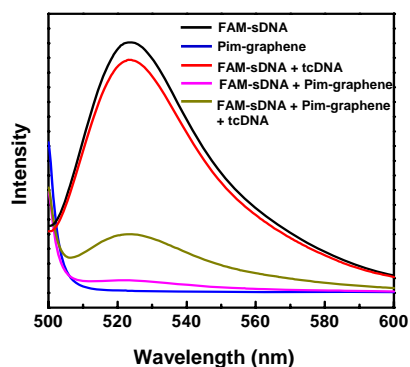


Fig. 4 Fluorescence spectra of FAM-sDNA (black curve), Pim-graphene (blue curve), FAM-sDNA in the presence of tcDNA (red curve), FAM-sDNA in the presence of Pim-graphene (magenta curve), and FAM-sDNA in the presence of Pim-graphene and tcDNA (dark yellow curve). FAM-sDNA concentration: 20 nM; tcDNA concentration: 50 nM; Excitation wavelength: 490 nm. Measurements were performed in 10 mM HEPES buffer containing 75 mM NaCl and 4 mM MgCl_2 (pH 7.4).

To demonstrate the universal application of our strategy, we functionalized Pim onto the other kind of CNS, i.e., graphene to form Pim-functionalized graphene (Pim-graphene) also by the surface-initiated atom transfer radical polymerization. The as-formed Pim-graphene was used as background signal platform for the fluorescence DNA sensor with FAM-labeled single strand DNA (FAM-sDNA) as the recognition unit (Fig. 4). As shown, the addition of 54 $\mu\text{g}/\text{mL}$ Pim-graphene results in the efficient fluorescence quenching of 20 nM FAM-sDNA, and further addition of 50 nM targeted-complementary DNA (tcDNA) leads to the recovery of the fluorescence, indicating that the Pim-graphene could be used as signal platform for fluorescence sensor (Fig. S4). The LOD ($S/N = 3$) was calculated to be 250 pM, which is 2 orders lower than the reported DNA sensor based on the graphene oxide as the signal platform.^{1a} This result essentially suggests that the present strategy is universal for the different kinds of CNS and biorecognition units.

In summary, we have demonstrated a new strategy to improving the fluorescence detection limit by enhancing the energy transfer efficiency between carbon nanostructures and fluorescent dye. Based on this, a highly sensitive method for thrombin detection was developed by using Pim-functionalized CNS as a low background signal platform. To the best of our knowledge, the method demonstrated here possesses the lowest detection of limit for thrombin detection based on fluorescence technique. Moreover, the strategy could be extended to other

kinds of CNS and recognition units. This work not only provides a new method for effective detection of thrombin but also opens a way to the design of novel methods for improving the sensor performance by, for example, rationally designing the surface chemistry of the CNS.

This research was financially supported by the NSF of China (Grants No. 21321003, 21210007, and 91213305 for L.M., 21322503 for P.Y., and 21275123 for J. F.), the National Basic Research Program of China (973 programs, 2010CB33502), and the "Strategic Priority Research Program" of the Chinese Academy of Sciences (Grant No. XDA09020100).

Notes and references

^a College of Chemistry, Xiangtan University, Xiangtan, Hunan 411105, China; ^b Beijing National Laboratory for Molecular Sciences, Key Laboratory of Analytical Chemistry for Living Biosystems, Institute of Chemistry, the Chinese Academy of Sciences (CAS), Beijing 100190, China

*Corresponding author: E-mails: yuping@iccas.ac.cn;

fei_junjie@xtu.edu.cn; lqmao@iccas.ac.cn; Fax: (86)-10-62559373.

† Electronic Supplementary Information (ESI) available: details of experimental section, CNT functionalization, and selectivity tests. See

DOI: 10.1039/b000000x/

- (a) C. Lu, H. Yang, C. Zhu, X. Chen and G. Chen, *Angew. Chem., Int. Ed.*, 2009, **121**, 4879-4881; (b) Z. Wang and Y. Lu, *J. Mater. Chem.*, 2009, **19**, 1788-1798; (c) J. Wang and X. Qu, *Nanoscale*, 2013, **5**, 3589-3600; (d) E. Morales-Narváez and A. Merkoçi, *Adv. Mater.*, 2012, **24**, 3298-3308; (e) H. Wang, R. Yang, L. Yang and W. Tan, *ACS Nano*, 2009, **3**, 2451-2460; (f) J. Kong, N. R. Franklin, C.W. Zhou, M. G. Chapline, S. Peng, K. Cho and H. J. Dai, *Science*, **287**, 622-625.
- (a) R. Polsky, R. Gill, L. Kaganovsky and I. Willner, *Anal. Chem.* 2006, **78**, 2268-2271; (b) J. Sharma, H. C. Yeh, H. Yoo, J. H. Werner and J. S. Martinez, *Chem. Commun.*, 2011, **47**, 2294-2296; (c) Z. Zhou, Y. Du and S. J. Dong, *Anal. Chem.*, 2011, **83**, 5122-5127; (d) H. Wei, B. L. Li, J. Li, E. K. Wang and S. J. Dong, *Chem. Commun.*, 2007, 3735-3737.
- R. Yang, J. Jin, Y. Chen, N. Shao, H. Kang, Z. Xiao, Z. Tang, Y. Wu, Z. Zhu, W. Tan, *J. Am. Chem. Soc.*, 2008, **130**, 8351-8358.
- (a) Y. Wang, L. Bao, Z. Liu and D. Pang, *Anal. Chem.*, 2011, **83**, 8130-8137; (b) H. Chang, L. Tang, Y. Wang, J. Jiang and J. Li, *Anal. Chem.*, 2010, **82**, 2341-2346; (c) R. Yang, Z. Tang, J. Yan, H. Kang, Y. Kim, Z. Zhu and W. Tan, *Anal. Chem.*, 2008, **80**, 7408-7413; (d) J. Liu, J. Li, Y. Jiang, S. Yang, W. Tan and R. Yang, *Chem. Commun.*, 2011, **47**, 11321-11323; (e) S. Zhu, Z. Liu, L. Hu, Y. Yuan and G. Xu, *Chem.-Eur. J.*, 2012, **18**, 16556-16561; (f) H. Li, Y. Zhang, T. Wu, S. Liu, L. Wang and X. Sun, *J. Mater. Chem.*, 2011, **21**, 4663-4668.
- (a) R. S. Swathi and K. L. Sebastiana, *J. Chem. Phys.*, 2008, **129**, 054703; (b) R. S. Swathi and K. L. Sebastiana, *J. Chem. Phys.*, 2009, **130**, 086101; (c) N. Nakayama-Ratchford, S. Bangsaruntip, X. Sun, K. Welsher, H. Dai, *J. Am. Chem. Soc.*, 2007, **129**, 2448; (d) Z. Zhu, Z. Tang, J. A. Phillips, R. Yang, H. Yang and W. Tan, *J. Am. Chem. Soc.*, 2008, **130**, 10856.